Cerebral Cortex, August 2018;28: 2810–2816

doi: 10.1093/cercor/bhx160
Advance Access Publication Date: 23 June 2017
Original Article

ORIGINAL ARTICLE

Alternative RNA Splicing Associated With Mammalian Neuronal Differentiation

Jiancheng Liu[1], Anqi Geng[1], Xiwei Wu[2], Ren-Jang Lin[2] and Qiang Lu[1]

[1]Department of Developmental and Stem Cell Biology, Beckman Research Institute of City of Hope, 1500 East Duarte Road, Duarte, CA 91010, USA and [2]Department of Molecular and Cellular Biology, Beckman Research Institute of City of Hope, 1500 East Duarte Road, Duarte, CA 91010, USA

Address correspondence to Qiang Lu. Email: qlu@coh.org

Abstract

Alternative pre-mRNA splicing (AS) produces multiple isoforms of mRNAs and proteins from a single gene. It is most prevalent in the mammalian brain and is thought to contribute to the formation and/or maintenance of functional complexity of the brain. Increasing evidence has documented the significant changes of AS between different regions or different developmental stages of the brain, however, the dynamics of AS and the possible function of it during neural progenitor cell (NPC) differentiation is less well known. Here, using purified NPCs and their progeny neurons isolated from the embryonic mouse cerebral cortex, we characterized the global differences of AS events between the 2 cell types by deep sequencing. The sequencing results revealed cell type-specific AS in NPCs and neurons that are important for distinct functions pertinent to the corresponding cell type. Our data may serve as a resource useful for further understanding how AS contributes to molecular regulations in NPCs and neurons during cortical development.

Key words: alternative splicing, cerebral cortex, neural progenitor cells, neuronal differentiation, RNA-seq

Introduction

Alternative precursor-mRNA (pre-mRNA) splicing (AS) is a key regulation in mammalian gene expression, generating diverse mRNA and protein isoforms. AS is especially prevalent in the mammalian brain and is thought to contribute to the establishment and/or maintenance of functional complexity of the brain (Li et al. 2007; Zheng and Black 2013; Raj and Blencowe 2015; Vuong et al. 2016). Indeed, multiple transcriptome studies of mammalian brains have uncovered significant differences of AS amongst various brain domains (Johnson et al. 2009; Ayoub et al. 2011), cortical layers (Belgard et al. 2011), developmental stages (Dillman et al. 2013; Yan et al. 2015), or neuron and glia cell types (Zhang et al. 2014). In addition, misregulation of AS is linked to specific neurological diseases (Faustino and Cooper 2003; Licatalosi and Darnell 2006), further suggesting the importance of AS in the normal function of the brain. To better understand the biological importance of AS in brain development and function, data documenting the in vivo status of AS during temporal progression of cellular specifications and between distinct neuronal cell lineages are essential, however, such data are still limited due to the technical difficulties in obtaining purified neural progenitor cells (NPCs) or distinct neuronal cell types. In a recently study, AS was examined in a cellular specification model of the mouse cerebral cortex, based on an Eomes-GFP transgenic reporter-mediated isolation of NPC and neuron populations (Zhang et al. 2016). While the study identified many differentially spliced genes between the 2 cell populations, the possible inclusion of other types of cells within the isolated Eomes-GFP negative NPC population might limit identification of the full scope of differential AS events between NPCs and neurons during cortical neurogenesis. We previously designed a dual reporter strategy by labeling NPCs with GFP and differentiated daughter neurons with RFP in transgenic animals to enable effective simultaneous isolation of NPCs and neurons from the embryonic cortex (Wang et al. 2011; Hahn et al. 2013). Using this system, we investigated the

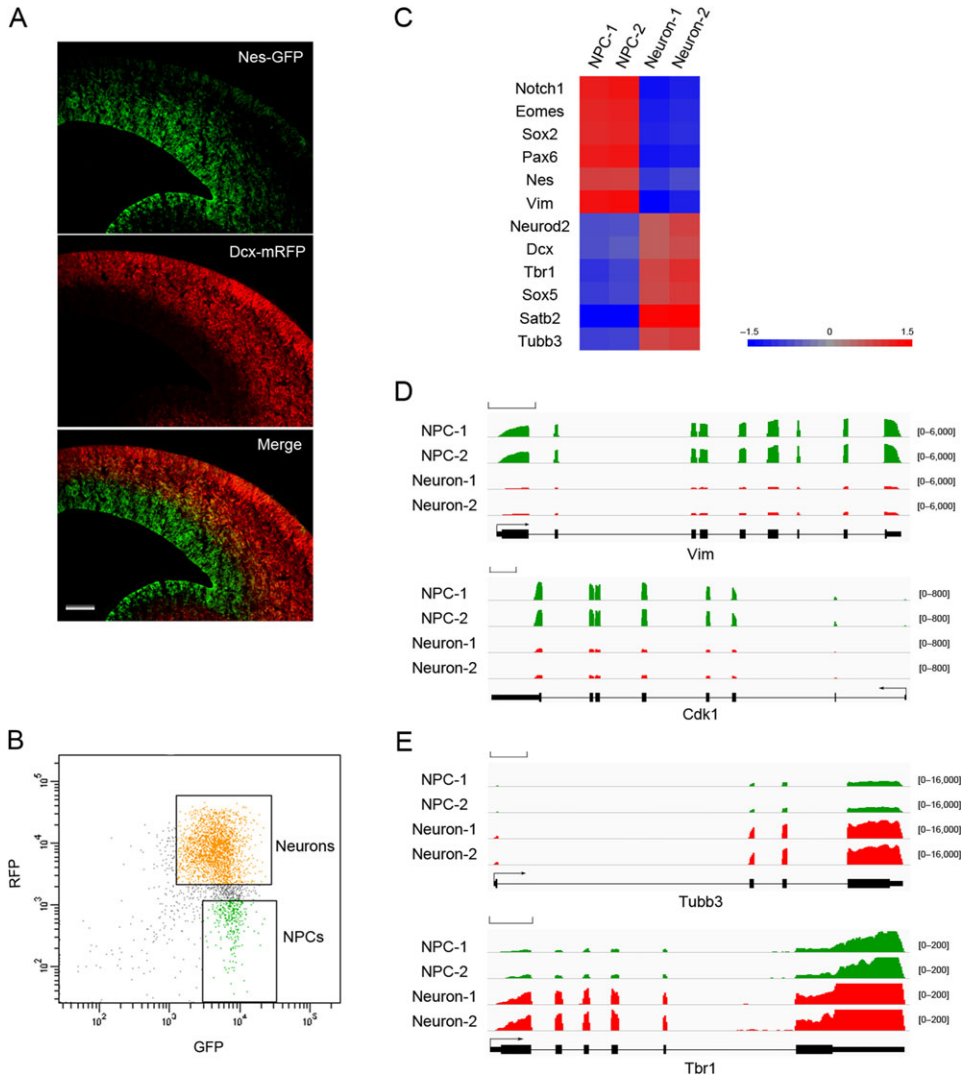

Figure 1. RNA-seq of purified neural progenitor cells (NPC) and neurons. (*A*) Images of brain sections from the double reporter transgenic mouse showing labeling of NPCs with Nestin-EGFP and neurons with Dcx-mRFP. Scale bar: 100 μm. (*B*) Fluorescence-activate cell sorting (FACS) profile of dissociated cortical cells derived from the E15.5 Nestin-EGFP/Dcx-mRFP embryos. Neural progenitor cells were GFP^+RFP^- cells. Daughter neurons were double positive due to carryover of GFP from NPCs. (*C*) Heatmap showing mRNA expression of NPC and neuron markers in each sample. NPC-1, -2 and Neuron-1, -2 represent duplicate samples for NPCs and neurons, respectively. (*D* and *E*) Representative marker gene tracks for NPCs (*D*) and neurons (*E*). The numbers in the square brackets represent data ranges. Gene modes are shown below with arrows as transcription start sites (TSSs). Scale bar: 1 kb.

dynamics of AS comparing purified NPCs and neurons. We present results revealing cell type-specific AS in NPCs and neurons and the potential functional implications in cortical neurogenesis.

Materials and Methods

Animals

Nestin-GFP and Dcx-mRFP transgenic reporter mice were previously described (Wang et al. 2011; Hahn et al. 2013). The Dcx-mRFP reporter line can be obtained from The Jackson Laboratory, C57BL/6J-Tg(Dcx-mRFP)15Qlu/J (Stock# 24905). Animal procedures were approved by the Institutional Animal Care and Use Committee (IACUC) and were carried out in accordance with NIH guideline and the Guide for the Care and Use of Laboratory Animals.

FACS-Mediated Purification of Cortical NPCs and Neurons

Purification of E15.5 cortical cells using a double reporter strategy was done as previously described (Wang et al. 2011; Hahn et al. 2013). Briefly, heterozygous Nestin-GFP mice were bred with homozygous Dcx-mRFP mice to yield GFP/RFP double positive embryos. The cortices derived from the double positive embryos were dissociated by trituration in HBSS (Mediatech) with 5 mM of EDTA (Invitrogen) and 25 μg/mL of DNase I (Roche). Cells were washed once using HBSS with 12.5 μg/mL of DNase I and resuspended in DMEM/F12 (Mediatech) with 12.5 μg/mL of DNase I and 5% BSA (Sigma-Aldrich). FACS was performed with a 4-laser BD FACSAria™ III System (BD Biosciences). Cell debris and doublets were excluded with gating of forward scatter, side scatter and pulse width. Sorted cells were collected into DMEM/F12 with 5% BSA.

RNA-seq

NPCs and neurons purified from E15.5 cortical cells were accumulated in duplicate samples, and total RNAs were isolated using Trizol reagent (Invitrogen). RNA-seq was done by the Integrative Genomics Core at City of Hope. Paired End libraries were prepared, size selected, gel purified and sequenced using Illumina HiSeq2000 system following the manufacturer's protocols (Illumina).

RNA-seq Data Analysis

The paired-end reads were aligned to mm9 genome assembly using Tophat v2 with default settings. In total, 37–40 millions of reads were sequenced with all samples. In one sample of NPCs, out of 39 006 345 aligned reads, 73.6% were mapped to exon region of RefSeq genes and there are 319 183 reads spanning exon junctions. In one sample of neurons, 73.3% of 37 748 810 aligned reads were aligned to exon regions, and 324 689 reads spanning exon junctions. The alternative splicing (AS) events were identified using MATS v3.0.8 with default settings. AS events with false discovery rate (FDR) ≤ 0.05 and the absolute value of inclusion level difference (|IncLevelDifference|) ≥ 0.1 were considered significant.

Results

We isolated NPCs and neurons from the embryonic day 15.5 (E15.5) cortices of the Nestin-GFP/Dcx-mRFP reporter mice (Fig. 1*A* and *B*). Total RNA from duplicate cell samples were extracted and pair-end deep RNA sequencing was performed. Analyses of the sequencing data confirmed specific expression of NPC markers and neuron markers in the respective cell population (Fig. 1*C*), consistent with our previous transcriptome study of purified NPCs and neurons by microarray (Wang et al. 2011). In addition, the data showed that the sequenced reads were mostly mapped to exons and that duplicate samples were highly consistent (Fig. 1*D* and *E*).

To identify differential AS between NPCs and neurons, we applied multivariate analysis of transcript splicing (MATS) to the sequencing data. By setting the FDR ≤ 0.05 and the absolute value of inclusion level difference (|IncLevelDifference|) ≥ 0.1, we identified 84 and 176 differential skipped exons (SE) from NPCs and neurons, respectively (Fig. 2*A*). Table 1 listed the NPC-specific skipped exon events. We also identified other types of splicing forms, such as retained intron (RI), alternative 5′ splice site (A5SS), alternative 3′ splice site (A3SS) and mutually exclusive exons (MXE). These differential splicing events were summarized in Figure 2*A* and detailed information of genes/events was included in the Supplementary Table S1. Figure 2*B–D* illustrated several examples of genes showing differential AS between NPCs and neurons. Dst and Map3k7 have one exon (green rectangular box) expressing higher in NPCs while relatively low in neurons (Fig. 2*B*), indicating this exon was mostly skipped in neurons comparing with NPCs. An exon in St7 and Dtnb (red rectangular box) was mainly present in neurons but was skipped in NPCs (Fig. 2*C*). In all cases, other adjacent exons were expressed at similar levels in both cell types. Ablim1 was identified as SE both in NPC and in neuron groups. The Ablim1 gene track showed one exon (green rectangular box) highly expressed in NPCs and one nearby exon (red rectangular box) primarily expressed in neurons (Fig. 2*D*). These results suggested that the identified AS events reflected differential exon expression levels between NPCs and neurons based on the sequencing data.

A

Alternative splicing types	FDR <= 0.05 & |IncLevelDifference|>= 0.1	
	NPC	Neuron
Skipped exon (SE)	84 (79.2%)	176 (84.6%)
Retained intron (RI)	1 (0.9%)	7 (3.4%)
Alternative 5' splice site (A5SS)	2 (1.9%)	6 (2.9%)
Alternative 3' splice site (A3SS)	4 (3.8%)	10 (4.8%)
Mutually exclusive exon (MXE)	15 (14.2%)	9 (4.3%)

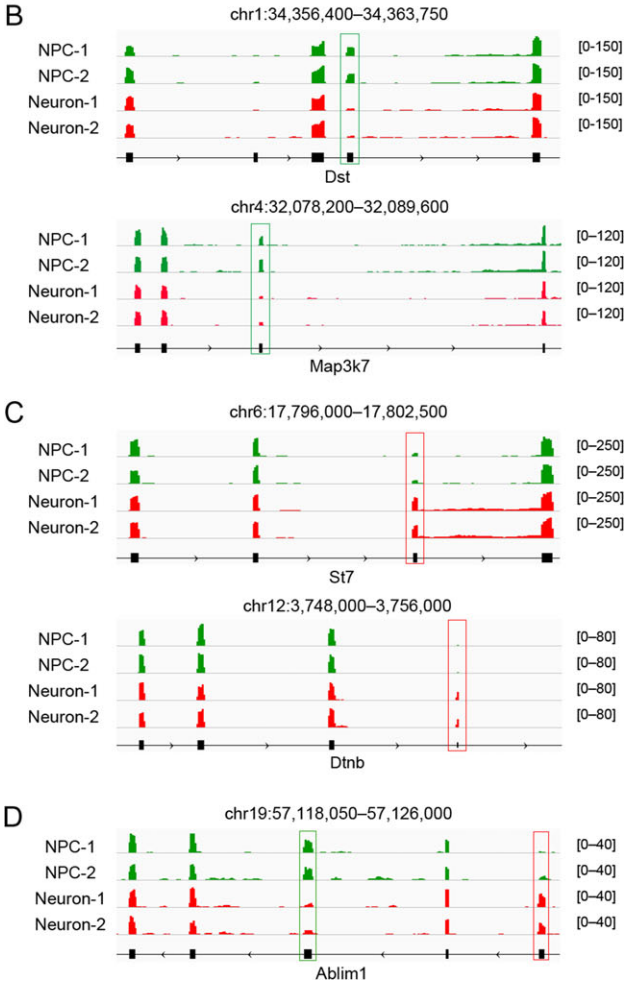

Figure 2. Alternative splicing events identified in NPCs and neurons. (*A*) Summary of alternative splicing events in NPCs and neurons. Numbers stand for cases of each event and percentages in brackets represent the percentage found of each event in that cell type. Black filled boxes represent constitutive exons, while empty boxes represent alternative exons. Blue and red lines represent splice junctions. FDR, false discovery rate. |IncLevelDifference|: absolute value of inclusion level difference. (*B–D*) Representative gene tracks for differential AS events specifically occurred in NPCs (*B*), neurons (*C*), or both cell types (*D*). Green rectangular boxes show NPC-specific events and red rectangular boxes indicate neuron-specific events. The numbers in the square brackets represent data ranges. The numbers on the top of tracks demonstrate the chromosomal locations of gene regions. Partial modes of genes are shown below with arrows indicate transcription directions.

Table 1 Neural progenitor cell-specific skipped exon (SE) events. The events were selected by FDR ≤ 0.05 and IncLevelDifference ≥ 0.1

Gene symbol	Chr	Strand	Exon start[a]	Exon end	FDR	IncLevelDifference	Gene symbol	Chr	Strand	Exon start[a]	Exon end	FDR	IncLevelDifference
Macf1	chr4	–	123 074 336	123 074 663	7.01E-08	0.641	Rif1	chr2	+	51 929 766	51 929 845	0.013097774	0.281
Dennd5a	chr7	–	117 078 995	117 079 067	5.85E-05	0.634	Mark3	chr12	+	112 890 168	112 890 195	0.000210272	0.277
L3mbtl3	chr10	–	26 063 982	26 064 057	7.12E-07	0.588	Bnip2	chr9	+	69 852 112	69 852 148	3.57E-08	0.275
Phf21a	chr2	+	92 191 988	92 192 021	1.40E-07	0.585	4833439L19Rik	chr13	–	54 665 870	54 665 982	5.93E-06	0.273
Sema6c	chr3	+	94 975 712	94 975 808	0.033364772	0.575	Bag6	chr17	+	35 279 442	35 279 550	3.13E-05	0.273
Fbxw7	chr3	+	84 668 058	84 668 122	0.030606885	0.572	Map4	chr9	+	109 983 924	109 984 114	0.015760831	0.266
Dnajb4	chr3	–	151 856 340	151 856 582	0.000531728	0.526	Cadm1	chr9	+	47 626 816	47 626 900	0.000318885	0.264
Ptprs	chr17	–	56 568 521	56 568 580	3.71E-11	0.518	Smarce1	chr11	–	99 086 034	99 086 456	0.041041541	0.254
Ap1ar	chr3	–	127 518 513	127 518 612	0	0.517	4833439L19Rik	chr13	–	54 665 875	54 665 982	3.15E-06	0.253
Lmo7	chr14	+	102 330 388	102 330 497	4.13E-06	0.496	Spag9	chr11	+	93 974 576	93 974 615	0.000185435	0.249
Tpm3	chr3	+	89 894 934	89 895 013	0.005602015	0.488	Pex2	chr3	–	5 562 668	5 562 732	2.69E-06	0.244
Ablim1	chr19	–	57 121 414	57 121 561	0.032365799	0.481	Dtwd1	chr2	+	125 984 145	125 984 289	0.010579952	0.244
Gphn	chr12	+	79 594 936	79 595 044	1.74E-07	0.48	Gatad2a	chr8	–	72 436 062	72 436 137	0.046675106	0.235
Prepl	chr17	–	85 487 679	85 488 215	0.001299817	0.475	Zfp942	chr17	–	22 078 692	22 078 817	0.028913391	0.233
Erc1	chr6	–	119 663 697	119 663 829	0.013567908	0.473	Atxn2	chr5	+	122 263 393	122 263 562	0.01290303	0.231
Ablim1	chr19	–	57 121 414	57 121 555	0.023845043	0.47	Mpzl1	chr1	–	167 531 880	167 531 986	0	0.23
Tmem176b	chr6	–	48 790 359	48 790 452	0.033717499	0.452	Usp14	chr18	–	10 017 988	10 018 093	0.009657061	0.224
Tmem63b	chr17	–	45 815 911	45 815 950	0.004671748	0.436	Eif4a2	chr16	+	23 112 423	23 112 530	0	0.223
Agfg1	chr1	+	82 876 582	82 876 702	6.77E-14	0.43	Prpf40a	chr2	–	53 018 296	53 018 350	8.14E-07	0.219
Myo5a	chr9	+	75 040 190	75 040 271	1.05E-06	0.429	Tecr	chr8	–	86 097 309	86 097 354	2.88E-12	0.213
Clip1	chr5	–	124077302	124077419	1.85E-05	0.429	App	chr16	–	85043820	85043988	8.19E-08	0.211
Map3k7	chr4	+	32 081 848	32 081 929	0.000449105	0.429	Lrrc49	chr9	–	60 528 311	60 528 509	0.029106763	0.209
Prepl	chr17	–	85 487 679	85 487 779	0.00797855	0.427	Dlgap4	chr2	+	156 573 758	156 574 156	2.23E-07	0.207
Immt	chr6	+	71 802 759	71 802 861	0.015399879	0.427	Zc3h14	chr12	+	100 018 257	100 018 490	8.20E-05	0.206
Dst	chr1	+	34 360 265	34 360 376	1.24E-09	0.425	Ktn1	chr14	+	48 324 094	48 324 163	0.002490497	0.198
Ubn1	chr16	+	5 081 986	5 082 076	0.04928753	0.421	Mtmr2	chr9	+	13 564 861	13 564 932	0.010953235	0.188
Sec16a	chr2	–	26 269 198	26 269 258	0.049598034	0.407	4833439L19Rik	chr13	–	54 665 545	54 665 633	9.16E-06	0.177
Ptprz1	chr6	+	22 974 713	22 974 734	0.001036352	0.397	Chtop	chr3	–	90 306 037	90 306 175	5.03E-06	0.16
Slmap	chr14	–	27 235 688	27 235 778	0.00226506	0.392	Ttc14	chr3	+	33 702 371	33 702 527	0.04928753	0.157
Fgfr1op2	chr6	+	146 541 155	146 541 269	1.45E-05	0.385	Gpm6b	chrX	+	162 823 322	162 823 413	0	0.156
Atxn2	chr5	+	122 231 341	122 231 551	0.002076189	0.371	Dlgap4	chr2	+	156 574 067	156 574 156	1.59E-09	0.146
Cyfip1	chr7	+	63 153 607	63 153 761	4.45E-07	0.365	Hp1bp3	chr4	+	137 777 440	137 777 638	0.00842253	0.142
Pbrm1	chr14	+	31 927 034	31 927 190	8.14E-07	0.362	Arfrp1	chr2	–	181 095 705	181 095 776	0.027669211	0.142
Akap9	chr5	+	3 954 396	3 954 450	0	0.356	Pbrm1	chr14	+	31 927 034	31 927 190	0.04376854	0.141
Pbrm1	chr14	+	31 923 600	31 923 765	0.011081276	0.349	Atp6v1h	chr1	+	5 091 150	5 091 204	0.000467451	0.132
Trp53bp1	chr2	–	121 054 323	121 054 443	0.000389815	0.329	Lrrfip1	chr1	+	92 999 823	92 999 895	0.014187386	0.131
Sgce	chr6	–	4 640 468	4 640 495	0.008825813	0.329	Erc1	chr6	–	119 728 005	119 728 089	0.000393889	0.129
Bptf	chr11	–	106 956 315	106 956 504	0.00961622	0.322	Pja2	chr17	–	64 647 064	64 647 250	0.008826884	0.128
Trim33	chr3	+	103 157 489	103 157 540	0.023808039	0.309	Zdhhc6	chr19	–	55 377 047	55 377 094	0.000185435	0.117
Eml4	chr17	+	83 824 597	83 824 771	3.66E-06	0.3	Hpf1	chr8	+	63 374 257	63 374 447	0.003325292	0.116
Pitpnb	chr5	+	111 814 539	111 814 624	2.12E-08	0.286	Map3k7	chr4	+	32 081 848	32 081 985	0.006226153	0.107
Banp	chr8	+	124 544 418	124 544 544	0.046858838	0.282	Tia1	chr6	+	86 373 599	86 373 665	0.022490662	0.1

[a]Exon start count from 0 base

Note: Chr, chromosome; FDR, false discovery rate; IncLevelDifference, inclusion level difference.

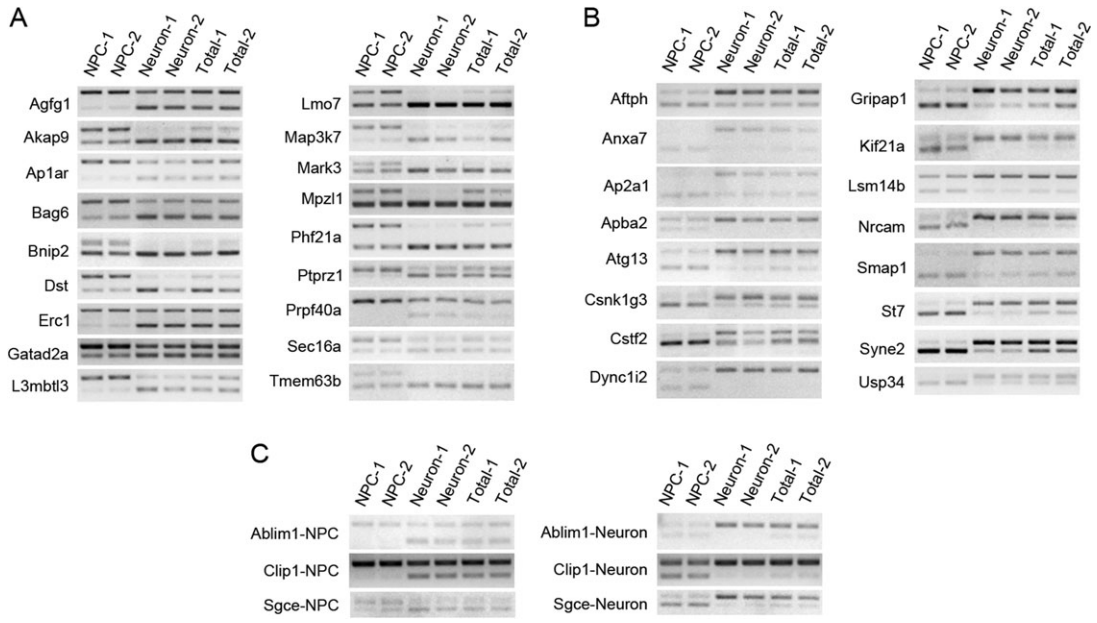

Figure 3. Validation of the AS events in E15.5 NPCs and neurons by RT-PCR. (*A*) 18 NPC-specific SE events were tested. All showed the upper PCR bands (sequence including the alternatively used exon by NPCs) either being detected specifically in NPC samples or showing relatively higher ratios in NPCs comparing to neurons. Total-1, -2 were unsorted duplicate samples of total cortical cells derived from the E15.5 cortices. (*B*) 16 neuron-specific SE events were tested. In all genes, the upper PCR bands (sequence including the alternatively used exon by neurons) either expressed specifically in neurons or had higher ratios in neurons comparing to NPCs. (*C*) The 3 genes having SE events in both cell types showed opposite patterns of the 2 differentially used exons in NPCs and in neurons.

To further validate the identified AS events, we performed reverse transcription-coupled polymerase chains reaction (RT-PCR). We selected 18 NPC-specific SE genes, 16 neuron-specific SE genes, as well as 3 genes showing SE events in both cell types. PCR primers spanning the skipped exons were specifically designed (Supplementary Table S2). Total RNAs were extracted from newly purified E15.5 NPCs and neurons in duplicates. RNAs from total cortical cells derived from the E15.5 cortices without FACS sorting were used as control. Samples with the same amount of total RNA were then used for reverse transcription. The results showed that 18 NPC-specific SE genes all had the upper PCR bands (sequence including the alternatively used exon by NPCs) either being detected specifically in NPC samples or showing relatively higher ratios in NPCs comparing to neurons (Fig. 3*A*). On the other hand, 16 neuron-specific SE genes showed a reverse pattern: the upper PCR bands (sequence including the alternatively used exon by neurons) either expressed specifically in neurons or had higher ratios in neurons comparing to NPCs (Fig. 3*B*). The 3 genes having SE events in both cell types showed opposite patterns in NPCs and in neurons (Fig. 3*C*). All together, these RT-PCR results were consistent with the differential AS events between NPCs and neurons identified from deep sequencing.

To gain insights into the potential functions of the differential AS events, we performed DAVID bioinformatics analyses (DAVID 6.8). Gene ontology analyses showed that the top biological processes in neuron-specific AS were microtubule cytoskeleton organization, cell migration and nervous system development (Fig. 4*A* and *B*; Supplementary Table S3), functions important for morphogenesis and migration. The top biological processes in NPC-specific AS were retrograde transport (protein transport from endosome to Golgi), covalent chromatin modification and nervous system development (Fig. 4*A* and *B*; Supplementary Table S3), functions crucial for recycling of membrane proteins or gene expression regulation. KEGG pathway analyses showed that ErbB signaling pathway (*P*-value: 0.0051) was at the top in neuron-specific AS events (Fig. 4*C* and Supplementary Table S3). Within NPC-specific AS events, adherens junction pathway (*P*-value: 0.0015) was the main pathway highlighted (Fig. 4*C* and Supplementary Table S3).

Discussions

Using purified NPCs and progeny neurons from the embryonic mouse cortices, we examined the dynamics changes of AS between NPCs and neurons by deep sequencing. Our RNA-seq data uncovered over 200 differential AS events between the 2 cell types, with skipped exons (SE) the major form of AS event occurring in cortical neurogenesis. RT-PCR using RNAs isolated from purified NPCs and neurons further validated the specific AS events suggested by the sequencing results, providing a foundation for further study of the potential mechanism and function of these differential AS events in neurogenesis. Gene ontology analyses revealed some clues on what might be the function of these identified AS events. Among neuron-specific AS events, genes involved in microtubule cytoskeleton organization and cell migration were the most prominent. This suggested that neuron-specific AS might be involved in neuronal morphogenesis including neurite outgrowth, dendritogenesis, or synapse formation/plasticity. The top emergence of the ErbB pathway among neuron-specific AS appeared to be consistent with this thought. ErbB signaling pathway has been implicated in regulating the assembly of neural circuitry, myelination, neurotransmission, and synaptic plasticity (Mei and Nave 2014). Among NPC-specific AS events, genes involved in retrograde endosome to Golgi transport and covalent chromatin modification were the most prevalent. This indicated that NPC-specific AS might be involved in certain important functions of

A

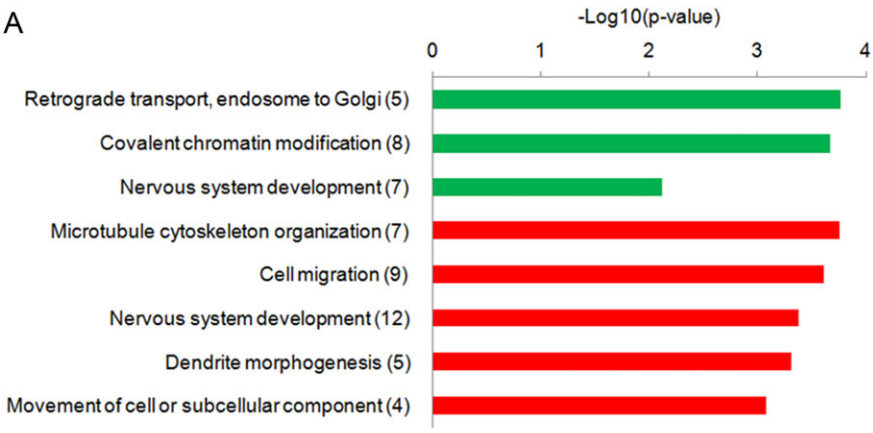

B

	Biological Process	Genes
NPC	Retrograde transport, endosome to Golgi	Spag9, Dennd5a, Arfrp1, Rab6a, Erc1
	Covalent chromatin modification	Hmgn3, Bag6, Smarce1, L3mbtl3, Phf21a, Pbrm1, Banp, Ubn1
	Nervous system development	App, Sema6c, Smarce1, Pex2, Cyfip1, Dlg3, Dock7
Neuron	Microtubule cytoskeleton organization	Ss18, Ptk2, Dclk2, Clasp1, Dock7, Clasp2, Mark3
	Cell migration	Ptprk, Ptprf, Sorbs2, Gpc6, Gsk3b, Abi2, Rps6kb1, Clasp2, Vav2
	Nervous system development	Ccdc64, Mef2a, Ptprf, Smarcb1, Pex2, Gsk3b, Smarcc2, Cyfip1, Dock7, Neo1, Kif2a, Kalrn
	Dendrite morphogenesis	Mef2a, Picalm, Abi1, Elavl4, Dvl1
	Movement of cell or subcellular component	Ptk2, Macf1, Abi2, Abi1

C

	KEGG Pathway	Genes	P-value
NPC	mmu04520:Adherens junction	Map3k7, Actn4, Sorbs1, Lmo7	0.001544
Neuron	mmu04012:ErbB signaling pathway	Ptk2, Gsk3b, Map2k4, Mapk9, Rps6kb1	0.005106
	mmu04910:Insulin signaling pathway	Sorbs1, Exoc7, Ptprf, Gsk3b, Mapk9, Rps6kb1	0.005159

Figure 4. Gene ontology of NPC- or neuron-specific SE events. (*A*) Top biological processes in NPC-specific (green bars, $P < 0.01$) and neuron-specific (red bars, $P < 0.001$) SE events. The numbers in brackets represent gene counts. (*B*) The genes included in each biological process (*A*) are listed. (*C*) KEGG pathways and genes in NPC-specific and neuron-specific SE events.

NPCs. Retrograde transport from endosome to Golgi regulates recycling of membrane proteins, which might be important for maintaining a proper proliferating state of NPCs, as cycling cells would require disassembly and reassembly of membrane proteins during cell divisions. Chromatin remodeling can impact gene expression and cell fate maintenance and has been implicated with important functions during neural progenitor development (Lomvardas and Maniatis 2016). The observation of adherens junction pathway as the top pathway in NPC-specific AS seemed to also agree with the idea. Proteins associated with adherens junctions are documented to regulate NPC functions in the developing cerebral cortex (Rasin et al. 2007; Lehtinen and Walsh 2011). While the specific functions and mechanisms of regulation of the characterized individual neuron- or NPC-specific AS events require further investigation, our data collectively indicated that the cell type-specific AS events in NPCs or neurons are functionally important for the corresponding cell type.

Using a Tbr2-EGFP transgenic reporter mouse strain, Zhang et al. (2016) recently isolated EGFP$^-$ (designated as NPCs) and EGFP$^+$ (designated as neurons) cells from the E14.5 mouse cerebral cortex and analyzed differential AS events between these 2 cell groups. A partial list of the identified AS events (63 genes/events) was presented in Zhang's study (Zhang et al. 2016), among which 26 events overlapped with our dataset (data not shown). Within the group of AS events (33 genes/events) that was validated by RT-PCR in Zhang's study, 16/33 events were found in our dataset (Supplementary Fig. S1). These partial overlaps of the differential AS events may be attributed to different populations of cells employed in RNA-seq, or different algorithms used for data analyses, or both. In Zhang's study, Tbr2-EGFP negative cells contained radial glial cells (RGCs, the primary progenitor cells of the cortex) as well as interneurons (Liu et al. 2016) and likely other cell types, while Tbr2-EGFP-expressing cells included projection neurons and intermediate

progenitor cells (IPCs). In this study, the Nestin-GFP/Dcx-mRFP dual reporter system provided co-isolation of NPCs (GFP^+RFP^- cells) and projection neurons (GFP^+RFP^+ cells), the former population contained both RGCs and IPCs. In summary, this study presented a systematic characterization of differential AS events between endogenous NPCs and their neuronal progeny. The data presented here may serve as a resource useful for further understanding how AS contributes to molecular regulations in NPCs and neurons during brain development.

Accession Number

Paired-end RNA-seq data of NPCs and neurons can be accessed at Gene Expression Omnibus (GEO) with accession number GSE96950.

Supplementary Material

Supplementary material is available at *Cerebral Cortex* online.

Funding

National Institute of Health (grants NS075393 from NINDS to Q.L.). In addition, research reported in this study included work performed in the Analytical Cytometry Core and Integrated Genomics Core supported by the National Cancer Institute under award number P30CA033572.

Notes

We thank Donna Isbell and Cirila Arteaga for assistance with animal breeding and care; Lucy Brown and Jeremy Stark and their staff for helping with cell sorting; Jinhui Wang for performing next-generation sequencing; Sika Zheng for critical reading of the article. *Conflict of Interest*: None declared.

References

Ayoub AE, Oh S, Xie Y, Leng J, Cotney J, Dominguez MH, Noonan JP, Rakic P. 2011. Transcriptional programs in transient embryonic zones of the cerebral cortex defined by high-resolution mRNA sequencing. Proc Natl Acad Sci USA. 108:14950–14955.

Belgard TG, Marques AC, Oliver PL, Abaan HO, Sirey TM, Hoerder-Suabedissen A, Garcia-Moreno F, Molnar Z, Margulies EH, Ponting CP. 2011. A transcriptomic atlas of mouse neocortical layers. Neuron. 71:605–616.

Dillman AA, Hauser DN, Gibbs JR, Nalls MA, McCoy MK, Rudenko IN, Galter D, Cookson MR. 2013. mRNA expression, splicing and editing in the embryonic and adult mouse cerebral cortex. Nat Neurosci. 16:499–506.

Faustino NA, Cooper TA. 2003. Pre-mRNA splicing and human disease. Genes Dev. 17:419–437.

Hahn MA, Qiu R, Wu X, Li AX, Zhang H, Wang J, Jui J, Jin SG, Jiang Y, Pfeifer GP, et al. 2013. Dynamics of 5-hydroxymethylcytosine and chromatin marks in mammalian neurogenesis. Cell Rep. 3:291–300.

Johnson MB, Kawasawa YI, Mason CE, Krsnik Z, Coppola G, Bogdanovic D, Geschwind DH, Mane SM, State MW, Sestan N. 2009. Functional and evolutionary insights into human brain development through global transcriptome analysis. Neuron. 62:494–509.

Lehtinen MK, Walsh CA. 2011. Neurogenesis at the brain-cerebrospinal fluid interface. Annu Rev Cell Dev Biol. 27: 653–679.

Li Q, Lee JA, Black DL. 2007. Neuronal regulation of alternative pre-mRNA splicing. Nat Rev. 8:819–831.

Licatalosi DD, Darnell RB. 2006. Splicing regulation in neurologic disease. Neuron. 52:93–101.

Liu J, Wu X, Zhang H, Qiu R, Yoshikawa K, Lu Q. 2016. Prospective separation and transcriptome analyses of cortical projection neurons and interneurons based on lineage tracing by Tbr2 (Eomes)-GFP/Dcx-mRFP reporters. Dev Neurobiol. 76:587–599.

Lomvardas S, Maniatis T. 2016. Histone and DNA modifications as regulators of neuronal development and function. Cold Spring Harb Perspect Biol. 8(7):pii:a024208. doi: 10.1101/cshperspect.a024208.

Mei L, Nave KA. 2014. Neuregulin-ERBB signaling in the nervous system and neuropsychiatric diseases. Neuron. 83: 27–49.

Raj B, Blencowe BJ. 2015. Alternative splicing in the mammalian nervous system: recent insights into mechanisms and functional roles. Neuron. 87:14–27.

Rasin MR, Gazula VR, Breunig JJ, Kwan KY, Johnson MB, Liu-Chen S, Li HS, Jan LY, Jan YN, Rakic P, et al. 2007. Numb and Numbl are required for maintenance of cadherin-based adhesion and polarity of neural progenitors. Nat Neurosci. 10:819–827.

Vuong CK, Black DL, Zheng S. 2016. The neurogenetics of alternative splicing. Nat Rev. 17:265–281.

Wang J, Zhang H, Young AG, Qiu R, Argalian S, Li X, Wu X, Lemke G, Lu Q. 2011. Transcriptome analysis of neural progenitor cells by a genetic dual reporter strategy. Stem Cells. 29:1589–1600.

Yan Q, Weyn-Vanhentenryck SM, Wu J, Sloan SA, Zhang Y, Chen K, Wu JQ, Barres BA, Zhang C. 2015. Systematic discovery of regulated and conserved alternative exons in the mammalian brain reveals NMD modulating chromatin regulators. Proc Natl Acad Sci USA. 112:3445–3450.

Zhang X, Chen MH, Wu X, Kodani A, Fan J, Doan R, Ozawa M, Ma J, Yoshida N, Reiter JF, et al. 2016. Cell-type-specific alternative splicing governs cell fate in the developing cerebral cortex. Cell. 166:1147–1162 e1115.

Zhang Y, Chen K, Sloan SA, Bennett ML, Scholze AR, O'Keeffe S, Phatnani HP, Guarnieri P, Caneda C, Ruderisch N, et al. 2014. An RNA-sequencing transcriptome and splicing database of glia, neurons, and vascular cells of the cerebral cortex. J Neurosci. 34:11929–11947.

Zheng S, Black DL. 2013. Alternative pre-mRNA splicing in neurons: growing up and extending its reach. Trends Genet. 29: 442–448.